CHAPTER II

INFLUENCE OF CHITOSAN BLENDED REDUCED GRAPHENE OXIDE NANOSHEETS FOR THE ELECTROCHEMICAL DETERMINATION OF p-AMINOPHENOL

2.1 INTRODUCTION

Phenols and its derivatives are treated as organic pollutant due to its serious deleterious effect on aquatic organisms. p- Aminophenol is used as an important intermediate in the synthesis of drugs. It is the hydrolytic degradation products that are dangerous to living things [1]. Due to its serious nephrotoxic and teratogenic effects, it is dangerous to humans and animals which cause irritation to eyes, skin and respiratory system. The accumulation of excess of acetaminophen causes severe fatal hepatoxicity, inflammation of the pancreas and skin rashes. On account of its high toxicity, the United States and European pharmacopeia's has limited the maximum content of p-AP in pharmaceuticals to 50 ppm [2-3]. Therefore, it is very important to develop a simple, sensitive and accurate detection method for the sensing of p-aminophenol. As a result of this, various methods have been proposed in the last few years such as HPLC method, capillary electrophoresis, micellar electro kinetic chromatography, nuclear magnetic resonance spectroscopy analysis, flow injection analysis with spectro photometric detection etc., Among all these methods electrochemical methods are considered to be effective methods due to its advantages like low cost, remarkable sensitivity, low-power requirement, quick detection etc.,[4-5]

Graphene oxide is a single layer of sp^2 hybridized carbon atoms, densely packed in a honey comb lattice. Owing to its extraordinary electronic transport property and high electrocatalytic activity, graphene oxide and its derivatives provides an effective sensing platform for the detection of biomolecules, toxins etc., the electrochemical reactions of analyte are greatly promoted on graphene film, resulting in the enhanced voltammetric response [6-7]. Chitosan (CS) is a linear β-1,4-linked polysaccharide natural bio polymer which has its reactive amino and hydroxyl groups in its linear high molar mass poly glucosamine chains that are amenable to chemical

modification. Due to its distinct chemical and biological properties, the chitosan-functionalized reduced graphene oxide electrode facilitates the electron transfer rate at the electrode surface through the π-π stacking interaction and electrostatic attraction, thus enhances the electrochemical performance for sensing applications [8-9]. In this chapter chitosan funtionalized reduced graphene oxide nanocomposites is synthesized by chemical reduction method. The synthesized nanocomposites are characterized using FT-IR, XRD, SEM, EDAX. The electrochemical sensing of p-Aminophenol is investigated using cyclic voltammetry.

2.2 EXPERIMENTAL PROCEDURE

2.2.1 Reagents

Graphite powder, Conc.sulphuric acid (98% H_2SO_4), potassium permanganate ($KMnO_4$), hydrogen peroxide solution (30% H_2O_2), sodium nitrate ($NaNO_3$), sodium hydroxide (NaOH) and chitosan, acetic acid, sodium borohydride ($NaBH_4$), p-aminophenol are of analytical grade, purchased from sigma Aldrich and are used as received without further purification.

2.2.2 Synthesis of Graphene oxide

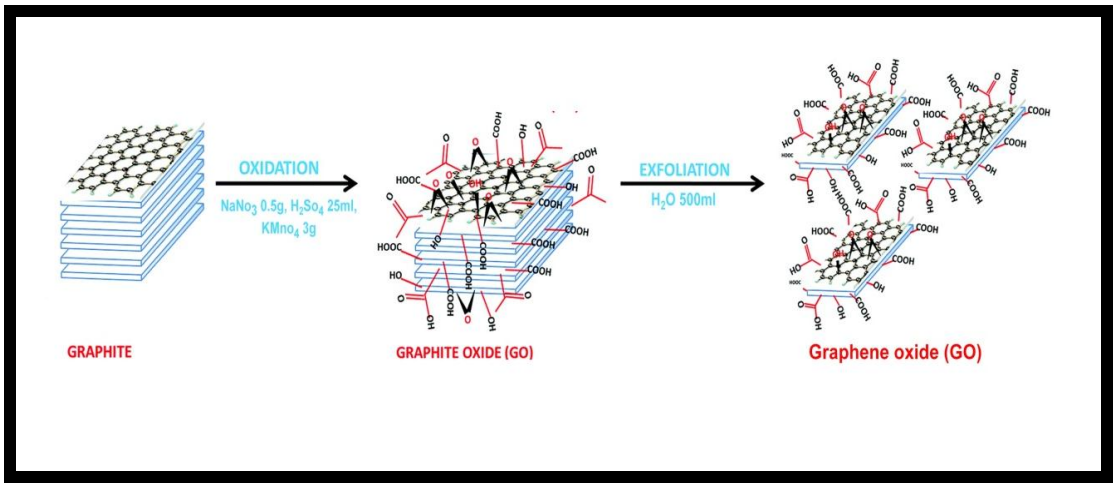

Figure 2.1 Schematic representation for synthesis of Graphene oxide

Graphene oxide (GO) is synthesized from natural graphite using modified hummer's method that includes both oxidation and exfoliation of graphite sheets. The schematic representation for synthesis of graphene oxide is shown in Figure 2.1.

The graphene oxide is synthesized by taking 1g of graphite powder and 0.5 g of sodium nitrate ($NaNo_3$) and are mixed in 25 ml of concentrated sulphuric acid (H_2SO_4) and kept under stirring for 1hour at room temperature. This is then followed by the gradual addition of 3 g of potassium permanganate ($KMnO_4$) under constant stirring by maintaining the temperature below 15°C to prevent overheating and explosion. The colour of the solution then becomes green indicating the formation of oxidizing agent. The temperature is then raised to 35°C and stirred continuously for 12 hours. The colour of the solution is turned into brown colour after 12 hours of continuous stirring which indicates that graphite has been successfully oxidized. The reaction mixture is diluted with the addition of 500 ml of distilled water in order to achieve better exfoliation. At the end of the reaction 5ml of 30% hydrogen peroxide (H_2O_2) solution is added to remove the excess of residual $KMnO_4$. The colour of the reaction mixture turns into yellow indicating the complete removal of $KMnO_4$ [10-11]. The solution is then left undisturbed for overnight and the resultant supernatant is filtered and washed with 10% HCl and distilled water until the solution reaches pH 7. The centrifuged solution is dried in oven at 60°C for 12 hours.

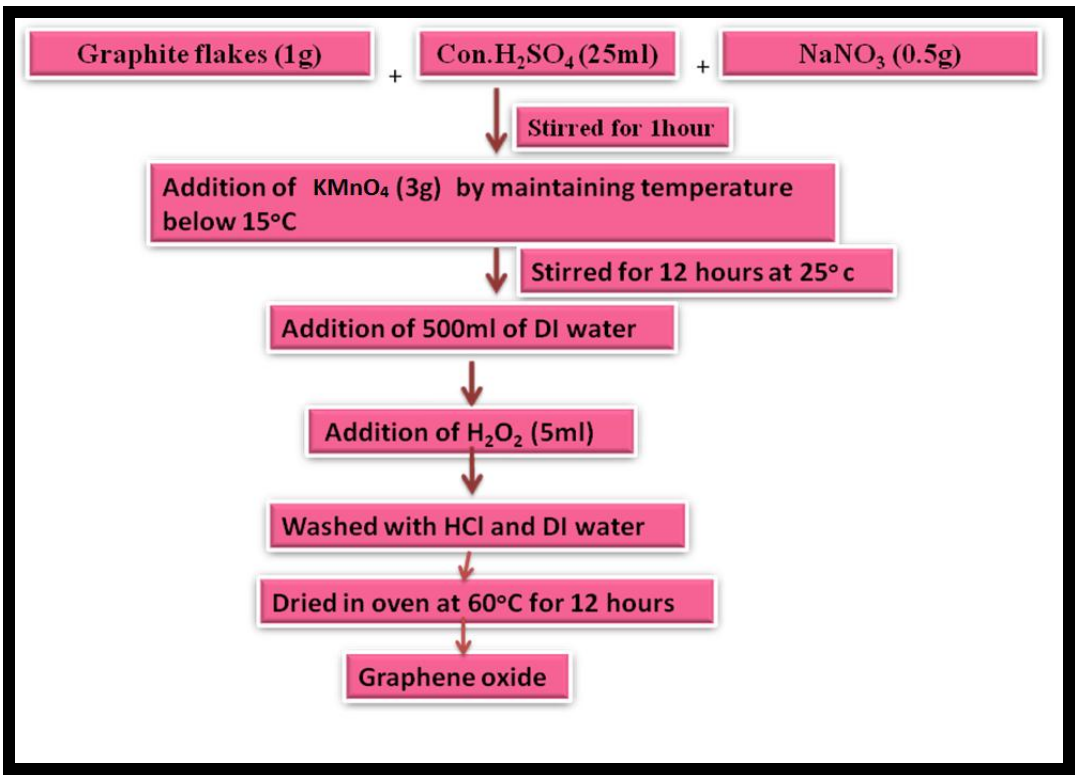

Figure 2.2 Flowchart for synthesis of graphene oxide

2.2.3 Synthesis of reduced graphene oxide/ chitosan nanocomposites

The reduced graphene oxide/chitosan (rGO/CS) nanocomposites is synthesized by chemical reduction method. In this typical synthesis, 50 mg of GO is dispersed in 25 ml of distilled water by ultrasonication for 1hour to form GO solution and 25 mg of chitosan is added into 2% acetic acid in water to prepare aqueous CS solution. The solution is stirred for 1hour at room temperature by maintaining the pH at 3. Thus the formed CS solution is added drop wise into the above dispersed GO solution. The temperature of the solution is then raised to 60°C and stirred for 1hour. Then 25 mg of sodium borohydride ($NaBH_4$) solution is stirred for 1hour at room temperature separately. The prepared $NaBH_4$ solution is added dropwise into the above reaction mixture. The solution is allowed to stir for 4 hours at 60°C and the resultant mixture is left undisturbed for overnight. The suspension is centrifuged and dried in oven for 60°C for 4 hours [12-13].

2.3 RESULTS AND DISCUSSION

2.3.1 FT-IR Spectral Analysis

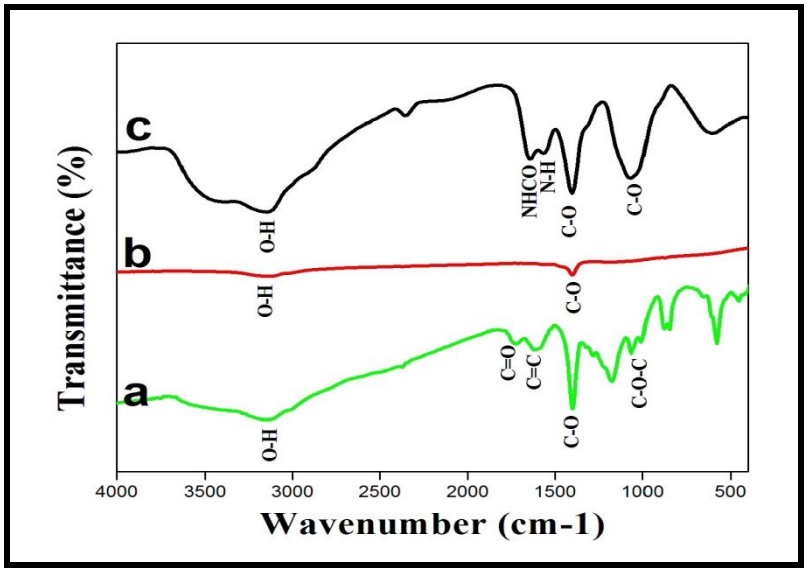

Figure 2.3 (a-c) FT-IR spectra of (a) GO (b) rGO (c) rGO/CS nanocomposites

FT-IR analysis is used to examine the presence of functional groups involved in the formation of RGO/CS. The FT-IR spectra for GO, rGO, rGO/CS

nanocomposites is shown in the Figure 2.3(a-c).The widest band formed around 3300 cm^{-1} to 3500 cm^{-1} corresponds to the O-H stretching vibrations of hydroxyl group. The low intensity band at 1620 cm^{-1} attributes to the C=C skeletal vibration of non-oxidized graphite which indicates that some of the graphite structures have retained even after the oxidation of graphite as shown in the Figure 2.3 (a). The sharp intense band at 1419 cm^{-1} can be attributed to C-O stretching vibrations of carboxyl groups. The characteristic bands of C=O stretching and bending vibrations of carboxylic acid are formed at 1733 cm^{-1} and 1221 cm^{-1}. Thus the presence of carbonyl, hydroxyl and epoxy groups attributes that graphite has been successfully oxidized into graphene oxide by modified Hummer's method [14-15].

The reduction of GO into rGO as in the Figure 2.3(b) shows two significant bands at 3300 cm^{-1} and 1419 cm^{-1} which corresponds to the O-H stretching vibrations of water molecules. Thus the decrease in the intensity of these bands clearly indicates the removal of oxygen groups from the graphene oxide. Moreover the disappearance of most of the absorption bands clearly indicates that graphene oxide has been successfully reduced into reduced graphene oxide [16].

It is evident from the rGO-CS spectrum that the disappearance of the band at 1733 cm^{-1} and the appearance of new band at 1640 cm^{-1} corresponding to NHCO stretching vibrations may be due to the reaction of carboxylic groups in GO with the NH_2 groups in CS. The band at 1056 cm^{-1} attributed to C-O stretching vibrations of primary alcohol is more intense than that of GO band at 1074 $cm^{-1}$and this may be due to the interaction of O-H groups of GO with CS. The characteristic band of secondary amide (N–H bending) is observed at 1544 cm^{-1} in GO spectrum shifted to lower wavelength at 1512 cm^{-1} in rGO-CS spectrum indicates the presence of newly formed amide bonds between GO and CS [17] . These results clearly show that CS has been binded completely with rGO.

2.3.2 XRD Structural Analysis

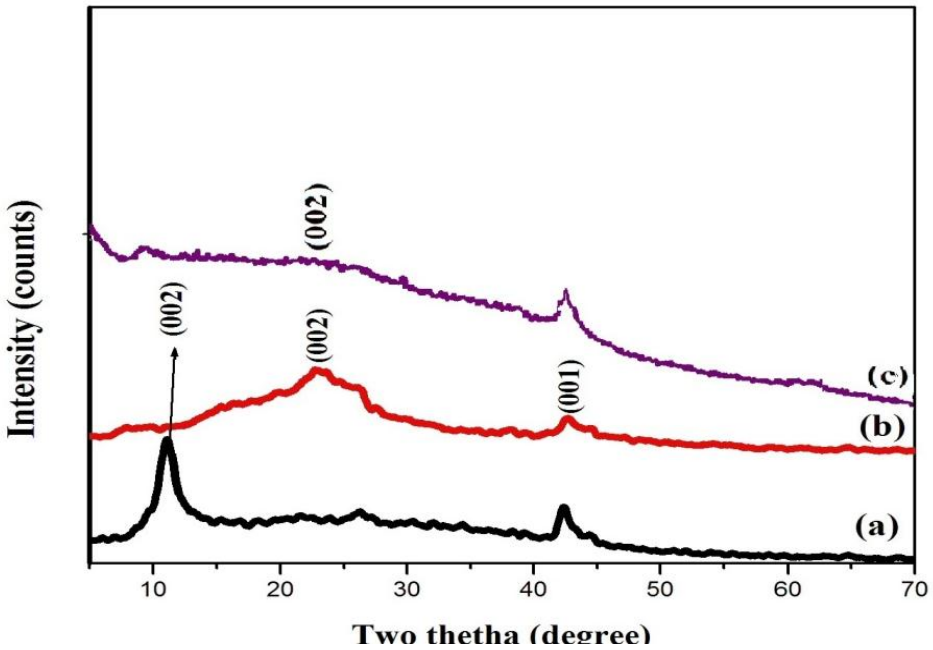

Figure 2.4 (a-c) XRD patterns for (a) GO (b) rGO (c) rGO/CS nanocomposites

The structure of the prepared nanocomposites is studied using X-Ray diffraction. The XRD pattern of GO, rGO and rGO/ CS nanocomposites are shown in the Figure 2.4 (a-c). The sharp peak at 11.42° corresponds to (002) plane of Graphene Oxide with an interlayer distance of 0.85 nm as shown in the Figure 2.4 (a). This indicates that the graphite is completely oxidized after the chemical oxidation by modified hummer's method. The small additional peak at 42° corresponds to the (001) plane and may be due to the incomplete oxidation of graphite [18].

It is observed from the Figure 2.4 (b) that after the reduction of graphene oxide into rGO, the sharp peak at 11.42° has shifted to 24° with an interlayer distance of 0.7 nm which clearly suggests the successful reduction of GO into rGO. The decrease in the interlayer distance in the diffraction peak of rGO clearly indicates the removal of oxygen functional groups from the planes of GO [19].

It is observed from the Figure 2.4 (c) that because of the blending of chitosan into rGO, a small diffraction peak appeared at 10.3° that corresponds to the plane of chitosan. The broad peak around 24 ° corresponds to the diffraction peak of reduced graphene oxide and broadening of the peak may be due to the amorphous nature of chitosan. Moreover the additional peak at 42° corresponds to the (001) plane which may be due to the incomplete oxidation of graphite [20-21]. It is further observed that the diffraction peak intensity of the chitosan blended reduced graphene oxide nanosheets is found to be very low compared with that of graphene oxide. These results clearly indicate that chitosan has been well blended into the rGO.

2.3.3 SEM analysis

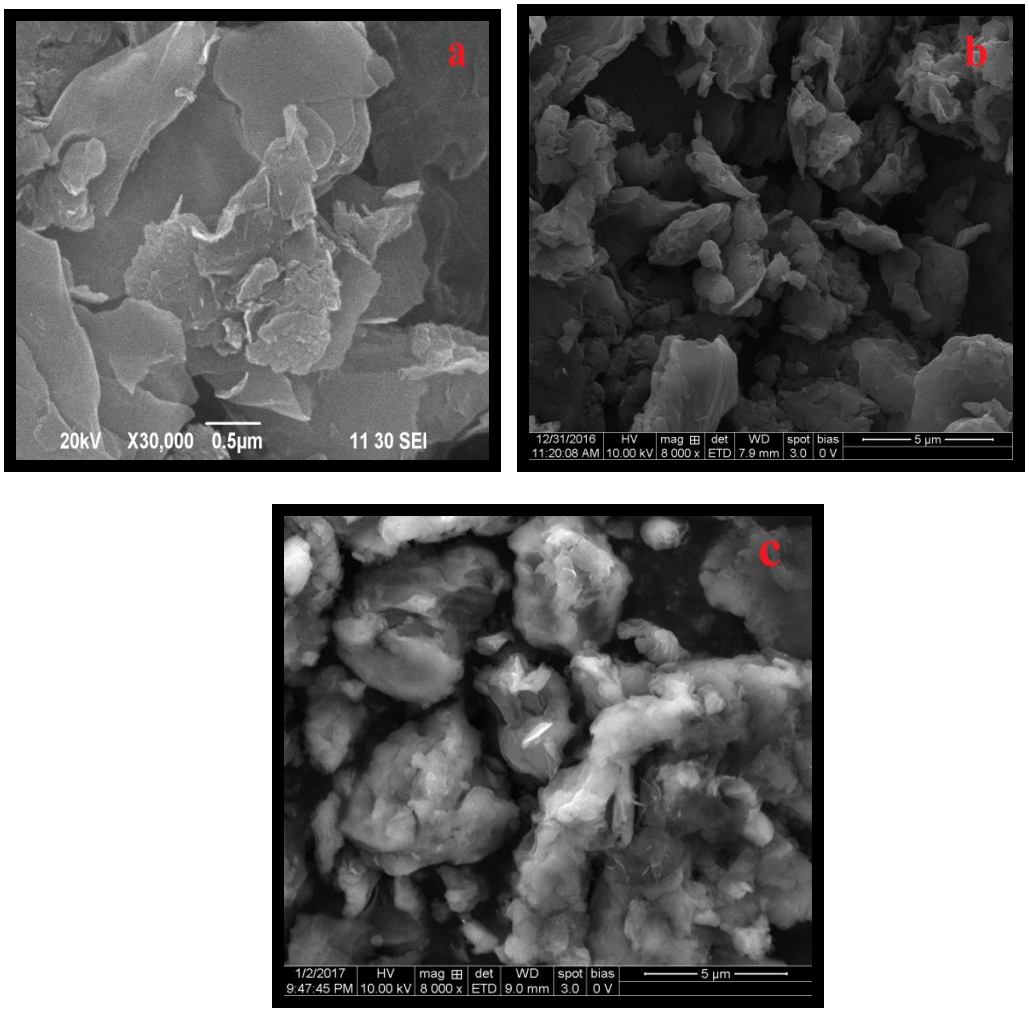

Figure 2.5 (a-c) SEM images of (a) GO (b) rGO and (c) rGO/CS nanocomposites

The morphological characterizations of the synthesized GO, rGO and rGO/CS nanocomposites are examined by Scanning electron microscopy**.** Figure 2.5 (a-c) shows the SEM images of GO, rGO and rGO/CS. It shows that the prepared graphene oxide is of thin sheets, significantly exfoliated and looks like a flat wrinkled leaf like structure with distinct edges and foldings as depicted in the Figure 2.5(a).It is further observed that the graphene oxide nanosheets are closely associated with each other [22-23]. Thus the wrinkled structure may be advantageous because of having high surface area of graphene oxide nanosheets that could prevent the sheets from collapsing back into graphitic structure.

Figure 2.5(b) shows the SEM images for the prepared reduced graphene oxide (rGO). It shows that the surface morphology of rGO is similar to that of GO. It is of thin sheets that are randomly aggregated with distinct edges, wrinkled surfaces and folding [24-25].

The soft white patches on the surface of rGO nanosheets as observed from the Figure 2.5 (c) attributes that chitosan has been fully covered on the surface of rGO and may be due to the formation of hydrogen bonding, which can interact with the hydroxyl, amino groups and carbonyl moieties in the graphene oxide sheets and chitosan respectively. This phenomena shows that chitosan has been strongly interacted with the reduced graphene oxide nanosheets which results in the enhancement of the properties of rGO/CS nanocomposites. [26-27].

2.3.4. Energy-Dispersive X-ray Analysis

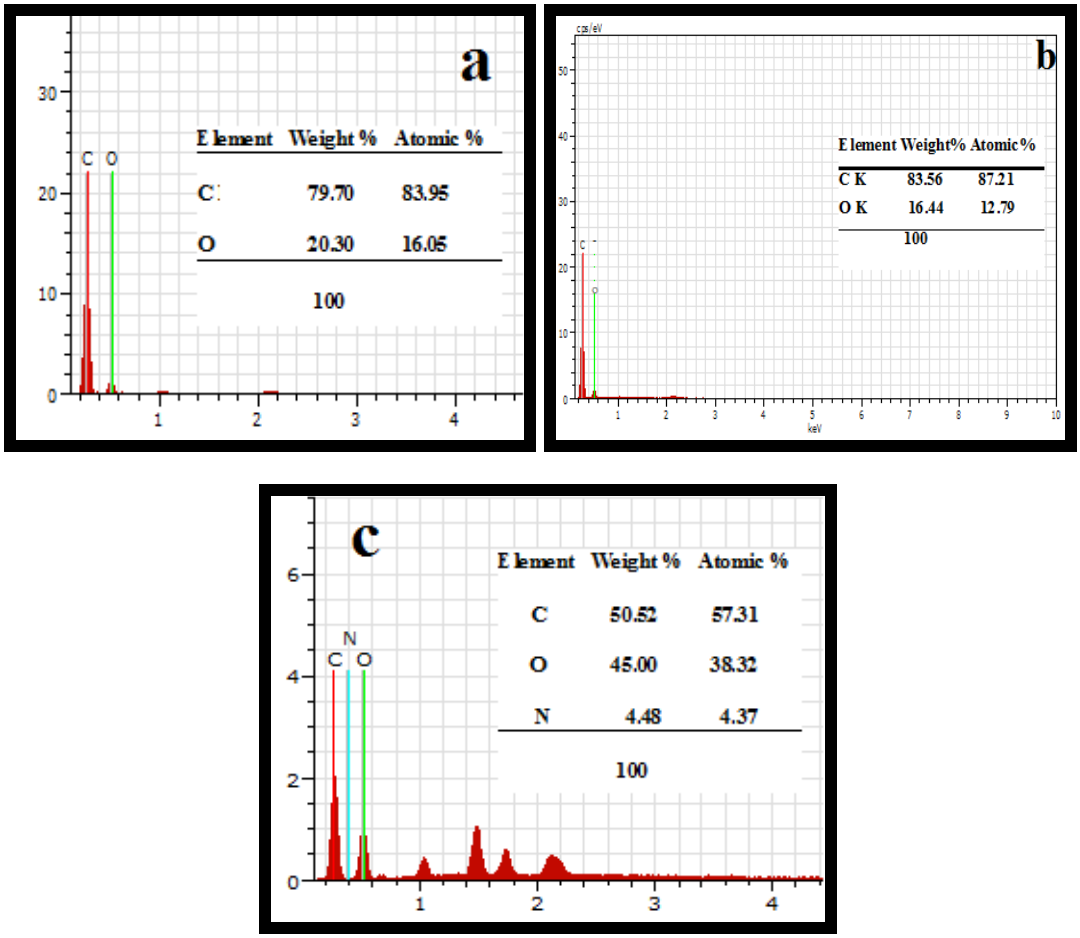

Figure 2.6 (a-c) EDAX spectra for (a) GO (b) rGO and (c) rGO/CS nanocomposites

The elemental analysis and chemical composition of the prepared nanocomposites is analyzed using Energy dispersive X-ray spectroscopic (EDAX) technique in the range between 0 and 20 KeV binding energy. In the Figure 2.6 (a-b), the presence of carbon and oxygen confirms the successful formation of graphene oxide and reduced graphene oxide [28]. The quantitative presence of carbon, oxygen and nitrogen as shown in Figure 2.6(c) [29,13], there by confirms the formation of rGO/CS nanocomposites .

The atomic and weight percentage of the elements are tabulated and shown in inset of Figure 2.6 (a-c). It is observed from the Figure 2.6 (a-b) that the percentage of oxygen in reduced graphene oxide is comparatively less than that of

graphene oxide therby indicating that oxygen elements have been removed during the reduction of graphene oxide. This confirms the successful formation of rGO as also evidenced from XRD analysis. It is further observed from the table that the O/C ratio of rGO/CS is higher than that of GO and the nitrogen element in rGO/CS is due to the NH_2 groups of CS. These results clearly attribute the incorporation of CS into the reduced graphene oxide.

2.4 ELECTROCHEMICAL RESPONSE OF p-AMINOPHENOL

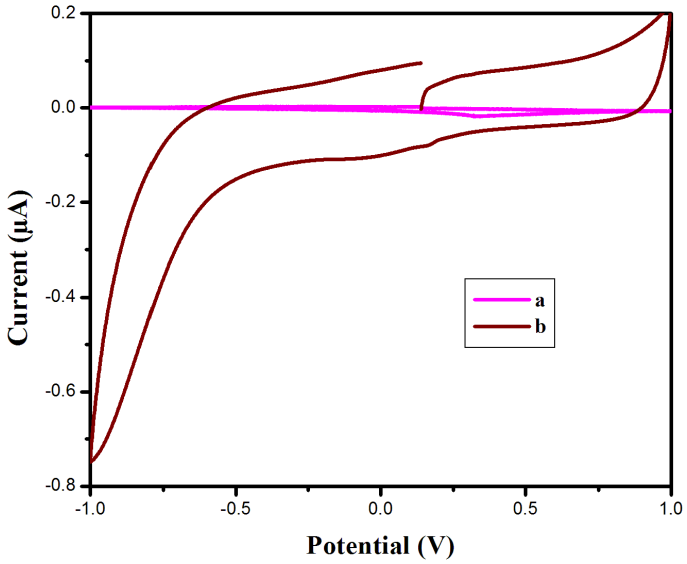

Figure 2.7 (a-b) Cyclic voltagramm curve for (a) GO/GCE (b) rGO/CS/GCE in presence of 10µM of p-Aminophenol in 0.1 M Phosphate buffer solution (PBS : pH 5) at a scan rate of 20 mV s^{-1}

The electrochemical measurements are carried out using electro chemical workstation. A three-electrode configuration is employed, consisting of a modified glassy carbon electrode (3mm in diameter) that serves as the working electrode and Ag/AgCl (3M KCl) and platinum wire serves as the reference and counter electrodes respectively. The electrochemical measurements are carried out in the electrolyte solution of 0.1 M phosphate buffer solution (PBS). The electro-chemical behaviour for the prepared GO and rGO/CS nanocomposites is measured using cyclic voltammetry (CV) and is carried out in PBS solution, at a potential range from -1 to 1 V with a scanning rate of 20 mV/s. Figure 2.7 (a-b) shows the Cyclic voltagramm

curve for GO and rGO/CS modified GCE. It is observed from the Figure 2.7 (a) that by the addition of 10µM of p-AP in 0.1 M Phosphate buffer solution, no redox peak is observed for GO modified GCE. In contrary a pair of weak redox peak is observed at a potential of about E_{pa} = 0.42V and E_{pc} = -0.009V is observed for rGO/CS modified GCE with peak current of about I_{pa} = 0.079µA and I_{pc} = -0.09µA. This remarkable increase in redox peak current of p-AP for rGO/CS modified GCE is due to the presence of chitosan [30, 3-4]. Due to its high adsorptive property, the rGO/CS nanocomposites increase its active sites which results in the larger accumulation of p-AP on the surface of nanocomposites. Thus the enhancement in strong electrocalatylic activity is because of the synergetic effect between rGO, CS and the high electron transfer rate of rGO/CS nanocomposites. Hence, these results show that rGO/CS nanocomposites exhibits high electrochemical property for the electrochemical detection of p-AP.

2.5 CONCLUSION

In this chapter, the polymer functionalized reduced graphene oxide nanocomposite is developed for the electrochemical detetction of p-AP. The graphene oxide is synthesized by modified Hummer's method and the chitosan functionalized reduced graphene oxide is synthesized by chemical reduction method. The synthesized rGO/CS nanocomposites is further characterized by FT-IR, XRD, SEM and EDAX analysis. XRD analysis shows the small diffraction peak at 10.3° corresponds to the plane of chitosan. The broadening of the peak at 24^{o} may be due to the amorphous nature of chitosan. FT-IR reveals that the band at $1640\,cm^{-1}$ corresponds to the NHCO stretching vibrations of amine groups of chitosan. The morphology of rGO/CS nanocomposites shows that the formation of white patches on the surface of flat wrinkled leaf like structure of rGO. The electro-chemical behaviour for the prepared GO and rGO/CS nanocomposites is investigated using cyclic voltammetry. The rGO/CS nanocomposites exhibits high redox peak current for p-AP compared to GO modified GCE. The high adsorptive property of chitosan and the high surface area of rGO results in the enhanced electrocatalytic activity of p-AP. Thus the rGO/CS modified GCE shows good electrocatalytic activity towards the detection of p-Aminophenol.

REFERENCES

1. Junjuan Qian, Depeng Zhang, Lirong Liu, Yinhui Yi, Mwenze Nkulu Fiston,Odoom Jibrael Kingsford and Gangbing Zhu, Carbon Spheres Wrapped with Molybdenum DisulfideNanostructure for Sensitive Electrochemical Sensing of 4-aminophenol, Journal of The Electrochemical Society, 165 (11) B491-B497 (2018).

2. S. Praveen Kumar, K. Giribabu, R. Manigandan, S. Munusamy, S. Muthamizh , A. Padmanaban, T. Dhanasekaran, R. Suresh, V. Narayanan, Simultaneous determination of paracetamol and 4-aminophenol based on poly(chromium Schiff base complex) modified electrode at nanomolar levels, Electrochimica Acta, vol.no.194 pg.no.116–126, (2016).

3. Graziella Scandurra, Arena Antonella, Carmine Ciofi, Gaetano Saitta and Maurizio Lanza, Electrochemical Detection of p-Aminophenol by Flexible Devices Based on Multi-Wall Carbon Nanotubes Dispersed in Electrochemically Modified Nafion, Sensors, 14, 8926-8939; doi:10.3390/s140508926, (2014).

4. Huanshun Yin, Qiang Ma, Yunlei Zhou, Shiyun Ai and Lusheng Zhu, Electrochemical behavior and voltammetric determination of 4-aminophenol based on graphene–chitosan composite film modified glassy carbon electrode, Electrochimica Acta 55,7,102–7108, (2010).

5. Yasemin Oztekin, Almira Ramana viciene, Arunas Ramanavicius, Electrochemical Glutathione Sensor Based on Electrochemically Deposited Poly-m-aminophenol, Electroanalysis, 23, No. 3, 701 – 709, (2011).

6. Elif Burcu Bahadır, Mustafa Kemal Sezgintürk, Applications of Graphene in Electrochemical Sensing and Biosensing, Trends in Analytical Chemistry, http://dx.doi.org/doi:10.1016/j.trac.2015.07.008, (2015).

7. Eluyemi M.S, Eleruja M.A, Adedeji A.V, Olofinjana B, Fasakin O, Akinwunmi O.O, Ilori O.O, Famojuro A.T, Ayinde S.A and Ajayi E.O.B, Synthesis and Characterization of Graphene Oxide and Reduced Graphene

Oxide Thin Films Deposited by Spray Pyrolysis Method. Graphene, 5, 143-154, (2016).

8. Duarte Moura, João F. Mano, Maria C. Paiva and Natália M. Alves, Chitosan nanocomposites based on distinct inorganic fillers for biomedical applications Sci. Technol. Adv. Mater. 17,627, (2016).

9. Richard Justin and Biqiong Chen, Strong and conductive chitosan–reduced graphene oxide nanocomposites for transdermal drug delivery, J. Mater. Chem. B, 2, 3759–3770, (2014).

10. Ayrat M. Dimiev and James M. Tour, Mechanism of Graphene Oxide Formation, ACS nano,8, 3, 3060-3068, (2014).

11. Gayathri, P. Jayabal, M. Kottaisamy and V. Ramakrishnan, Synthesis of few layer graphene by direct exfoliation of graphite and a Raman spectroscopic study AIP Advances 4, 027116 , https://doi.org/10.1063/1.486659 S,(2014).

12. Zhimin Luo, Dongliang Yang, Guangqin Qi, Lihui Yuwen, Yuqian Zhang, Lixing Weng, Lianhui Wang and Wei Huang, Preparation of Highly Dispersed Reduced Graphene Oxide Decorated with Chitosan Oligosaccharide as Electrode Material for Enhancing the Direct Electron Transfer of Escherichia coli ACS Appl. Mater. Interfaces. 7, 8539−8544, (2015).

13. Fatemeh Emadi, Abbas Amini, Ahmad Gholami,Younes Ghasemi, Functionalized Graphene Oxide with Chitosan for Protein Nanocarriers to Protect against Enzymatic Cleavage and Retain Collagenase Activity, Scientific Reports, 7,42258, DOI: 10.1038/srep42258, (2016).

14. Jianguo Song, Xinzhi Wang and Chang-Tang Chang, Preparation and Characterization of Graphene Oxide, Journal of Nanomaterials, (2014).

15. Neeru Sharma, Vikas Sharma, Yachana Jain, Mitlesh Kumari, Ragini Gupta, S. K. Sharma and K. Sachdev, Synthesis and Characterization of Graphene

Oxide (GO) and Reduced Graphene Oxide (rGO) for Gas Sensing Application, Macromolecular Symposia,376, 1700006, (2017).

16. Yuefang Zhang, Jia Liu, Yahong Zhang, Jin Liua and Yuping Duan, Facile synthesis of hierarchical nanocomposites of aligned polyaniline nanorods on reduced graphene oxide nanosheets for microwave absorbing materials, RSC Adv, 7, 54031, (2017).

17. Kosowska, Patrycja Domalik-Pyzik, Małgorzata Krok-Borkowicz and Jan Chłopek, Synthesis and Characterization of Chitosan/Reduced Graphene Oxide Hybrid Composites Karolina, Materials, 12, 2077; doi:10.3390/ma12132077, (2016).

18. Leila shahriary and anjali a. Athawale, Graphene oxide synthesized by using modified hummers approach, International Journal of Renewable Energy and Environmental Engineering, ISSN 2348-0157, Vol. 02, No. 01, (2014).

19. Changjing Fu, Guogang Zhao, Haijun Zhang, Shuang Li, Evaluation and Characterization of Reduced Graphene Oxide Nanosheets as Anode Materials for Lithium-Ion Batteries Int. J. Electrochem. Sci., 8, 6269 – 6280, (2013).

20. Xiaoming Yang, Yingfeng Tu, Liang Li, Songmin Shang and Xiao-ming Tao, Well-Dispersed Chitosan/Graphene Oxide Nanocomposites, ACS applied materials and interfaces, vol 2, no. 6, pg.no.1707–1713, (2010).

21. Hongqian Bao , Yongzheng Pan , Yuan Ping , Nanda Gopal Sahoo , Tongfei Wu , Lin Li , Jun Li and Leong Huat Gan, Chitosan-Functionalized Graphene Oxide as a Nanocarrier for Drug and Gene Delivery*7*, No. 11, 1569–1578, (2011).

22. Kobra Gerani, Hamid Reza Mortaheb, and Babak Mokhtarani, Enhancement in Performance of Sulfonated PES Cation-Exchange Membrane by Introducing Pristine and Sulfonated Graphene Oxide Nanosheets Synthesized through Hummers and Staudenmaier Methods, Polymer-plastics technology and engineering, vol.no 56, issue 5, 543–555, (2017).

23. O. Akgul , U. Alver and A. Tanrıverdi, Characterization of graphene oxide produced by Hummers method and its supercapacitor applications, AIP Conference Proceedings 1722, 280001, doi: 10.1063/1.4944280, (2016).

24. Sabina Drewniak, Roksana Muzyka, Agnieszka Stolarczyk, Tadeusz Pustelny, Michalina Kotyczka-Mora ´nska and Maciej Setkiewicz, Studies of Reduced Graphene Oxide and Graphite Oxide in the Aspect of Their Possible Application in Gas Sensors, Sensors, 16, 103, doi:10.3390/s16010 103, (2016).

25. Ning Cao and Yuan Zhang, Study of Reduced Graphene Oxide Preparation by Hummers Method and Related Characterization, Journal of nanomaterials, (2015)

26. Mona Mohseni and Hasan Tahermansouri, Development of a graphene oxide/chitosan nanocomposite for the removal of picric acid from aqueous solutions: study of sorption parameters, https://doi.org/10.1016/j. colsurfb.2017.10.019, (2017).

27. D. Depan, T. C. Pesacret and R. D. K. Misra, The synergistic effect of a hybrid graphene oxide–chitosan system and biomimetic mineralization on osteoblast functions, Biomater. Sci., 2, 264, (2014).

28. Zhihong Zhang, Xiaoming Fu, Kunzhen Li, Ruixue Liu, Donglai Peng, Linghao He, Minghua Wang, Hongzhong Zhang, Liming Zhou, One-step fabrication of electrochemical biosensor based on DNA-modified three-dimensional reduced graphene oxide and chitosan nanocomposite for highly sensitive detection of Hg(II), Sensors and Actuators B, 225,453–462, (2016).

29. N.I. Zaaba, K.L. Foo, U. Hashim, .J.Tan, Wei-Wen Liu, C.H. Voona, Synthesis of Graphene Oxide using Modified Hummers Method Solvent Influence, Science Direct, Procedia Engineering 184, 469 – 477, (2017).

30. Santhana Krishna Kumara and Shiuh-Jen Jianga, Chitosan-functionalized graphene oxide: A novel adsorbent an efficient adsorption of arsenic from aqueous solution, http://dx.doi.org/doi:10.1016/j.jece.2016.02.035, (2016).